

Resonance and absorption spectra of the Schwarzschild black hole for massive scalar perturbations: a complex angular momentum analysis

Yves Décanini,^{1,*} Antoine Folacci,^{1,2,†} and Bernard Raffaelli^{1,‡}

¹*Equipe Physique Théorique, SPE, UMR 6134 du CNRS et de l'Université de Corse, Université de Corse, Faculté des Sciences, BP 52, F-20250 Corte, France*

²*Centre de Physique Théorique, UMR 6207 du CNRS et des Universités Aix-Marseille 1 et 2 et de l'Université du Sud Toulon-Var, CNRS-Luminy Case 907, F-13288 Marseille, France*

(Dated: August 29, 2018)

We reexamine some aspects of scattering by a Schwarzschild black hole in the framework of complex angular momentum techniques. More precisely, we consider, for massive scalar perturbations, the high-energy behavior of the resonance spectrum and of the absorption cross section by emphasizing analytically the role of the mass. This is achieved (i) by deriving asymptotic expansions for the Regge poles of the S -matrix and then for the associated weakly damped quasinormal frequencies and (ii) by taking into account the analytic structure of the greybody factors which allows us to extract by resummation the physical information encoded in the absorption cross section.

PACS numbers: 04.70.-s, 04.50.Gh

I. INTRODUCTION

Since the pioneering paper of Matzner [1] inspired by a related but unpublished work of Hildreth [2], wave scattering and absorption by black holes is a topic which has been extensively studied due to (i) its mathematical interest because scattering theory is a branch of mathematical physics (see, e.g., Ref. [3]) which has found with black holes and curved spacetimes a new and rich field of activities, but also and above all due to (ii) its physical interest in connection with various fundamental or experimental aspects of classical and quantum gravity such as perturbation theory of black holes, gravitational wave theory, quasinormal modes and resonant scattering theory, weak and strong lensing, superradiance and instabilities, Hawking radiation, information paradox, holography and CFT correspondence, higher-dimensional field theories, analogue models of gravity... We refer to the monograph of Futterman, Handler and Matzner [4] and to references therein for the literature on wave scattering and absorption by black holes prior to 1988 and to Refs. [5–14] for a short and non-exhaustive list of papers on this subject published since this date and which, to our opinion, shed light on it from new and interesting points of view.

Of course, in the context of scattering and absorption by black holes, physicists have been mainly concerned with massless field theories with spin 0, 1/2, 1, 2 which are considered to be much more relevant, from a physical point of view, than massive ones. However, regularly since the seventies, some interesting articles dealing with massive field theories and considering, in particular,

the influence of the mass parameter on various aspects of scattering in the frequency domain (scattering resonances, bound states, cross sections, instabilities...) or in the time domain (late-time tails, instabilities...) have been published (see, e.g., Refs. [15–26]) and during the last decade an increasing number of papers dealing with these same topics appeared (see, e.g., Refs. [12, 27–44]).

In this paper, we shall consider the simple case of a massive scalar field propagating on the Schwarzschild black hole and we shall revisit two particular aspects of scattering by this gravitational background in the framework of complex angular momentum (CAM) techniques, i.e., in other words, by using the Regge pole machinery. (For a review of CAM techniques in scattering theory, we refer more particularly to the monograph of Newton [3] and for the use of these techniques in the context of black hole physics, we refer to Refs. [6, 7, 14, 45–50]). More precisely, we intend to describe the high-energy behavior of the scattering resonance spectrum and of the absorption cross section by emphasizing the role of the mass parameter. It should be noted that these two topics have been already considered by numerous authors [15, 19, 24, 26, 32, 36, 43] but precise descriptions have been only obtained from purely numerical analysis (see, however, Ref. [33] where an analytically solvable toy-model has been considered in order to understand the mass-dependence of the scattering resonance spectrum and a very recent paper by Hod [44] where the fundamental resonances of near-extremal Kerr black holes due to massive scalar perturbations are derived analytically). The CAM approach will permit us to go beyond numerical considerations and to understand analytically in term of the mass parameter well-known effects such as the migration of the complex quasinormal frequencies and the behavior of the absorption cross section. Of course, it is important to recall that Regge pole techniques are formally valid for “high” frequencies. As a consequence, they do not allow us to describe in the usual

*Electronic address: decanini@univ-corse.fr

†Electronic address: folacci@univ-corse.fr

‡Electronic address: raffaelli@univ-corse.fr

CAM framework the existence of the bound state spectrum [16, 20, 23, 25, 36, 43] which is an important aspect of the massive scalar field theory on the Schwarzschild black hole appearing for rather low frequencies.

Our article is organized as follows. In Sec. II, we shall first construct high-frequency asymptotic expansions for the Regge poles associated with the massive scalar field. We shall use two different approaches, both emphasizing the role played by the black hole photon sphere: (i) a powerful approach developed recently by Dolan and Ottewill in Ref. [47] which is based on a novel ansatz for the Regge poles and the associated Regge modes and (ii) a more traditional approach (see Refs. [48, 49] for previous applications to massless theories) based on the WKB method developed a long time ago by Schutz, Will and Iyer (see Refs. [51–55]) to study the resonant behavior of black holes. Then, from the Regge poles, we shall obtain the weakly damped quasinormal frequencies of the massive scalar field in term of the mass parameter. This will allow us to show explicitly that when the mass of the scalar field increases, the oscillation frequency of a quasinormal mode increases while its damping decreases. In Sec. III, we shall consider the absorption problem for the massive scalar field. From Regge pole techniques, we shall make a resummation of the absorption cross section and then provide a simple formula describing very precisely, at high energies, its behavior and emphasizing more particularly the role of the mass parameter and of the black hole photon sphere. We shall finally conclude this paper by briefly considering some possible generalizations of the present work. Throughout this paper, we shall use units such that $\hbar = c = G = 1$ and assume a harmonic time dependence $\exp(-i\omega t)$ for the massive scalar field.

II. REGGE POLES FOR THE MASSIVE SCALAR FIELD AND ASSOCIATED COMPLEX QUASINORMAL FREQUENCIES

A. Generalities and notations

In this subsection, we shall describe the first problem we intend to solve by using the CAM machinery and we shall also fix the main notations used in our article.

We first recall that the exterior of the Schwarzschild black hole of mass M is defined by the metric

$$ds^2 = -(1 - 2M/r)dt^2 + (1 - 2M/r)^{-1}dr^2 + r^2 d\sigma_2^2 \quad (1)$$

where $d\sigma_2^2 = d\theta^2 + \sin^2\theta d\varphi^2$ denotes the metric on the unit 2-sphere S^2 and with the Schwarzschild coordinates (t, r, θ, φ) which satisfy $t \in]-\infty, +\infty[$, $r \in]2M, +\infty[$, $\theta \in [0, \pi]$ and $\varphi \in [0, 2\pi]$.

In order to simplify discussions below and to interpret physically some of our results, it is also necessary to point out various aspects of scattering of massive (and massless) particles by the Schwarzschild black hole linked more or less directly with the existence of its photon

sphere at $r = 3M$ (see, e.g., Chap. 25 of Ref. [56] or, for more precisions, Chap. 3 of Ref. [57] and, for some of the notations we shall use, Ref. [12]). We consider a particle with rest mass μ and energy $\omega > \mu$ and we denotes by $p(\omega) = \sqrt{\omega^2 - \mu^2}$ and by $v(\omega) = p(\omega)/\omega$ the particle momentum and the particle speed at large distances from the black hole. We note, in particular, that

$$v(\omega) = \sqrt{1 - \frac{\mu^2}{\omega^2}}. \quad (2)$$

We recall that, associated with the parameter ω and for μ fixed, there exists a sphere located at $r = r_c(\omega)$ with

$$r_c(\omega) = 2M \left(\frac{3 + (1 + 8v^2(\omega))^{1/2}}{1 + (1 + 8v^2(\omega))^{1/2}} \right) \quad (3)$$

on which the massive particle can orbit the black hole on unstable circular (timelike) geodesics. We have $r_c(\omega) \in]3M, 4M[$. We also recall that the critical radius $r_c(\omega)$ defines a critical impact parameter

$$b_c(\omega) = \frac{M}{\sqrt{2}v^2(\omega)} \left[8v^4(\omega) + 20v^2(\omega) - 1 + (1 + 8v^2(\omega))^{3/2} \right]^{1/2}. \quad (4)$$

The black hole captures any particle sent toward it with an impact parameter $b < b_c(\omega)$ while particles with impact parameter $b > b_c(\omega)$ are scattered. As a consequence, for particles with rest mass μ and energy ω , the geometrical cross section of the Schwarzschild black hole is $\sigma_{\text{geo}}(\omega) = \pi b_c^2(\omega)$ or reads more explicitly

$$\sigma_{\text{geo}}(\omega) = \frac{\pi M^2}{2v^4(\omega)} \left[8v^4(\omega) + 20v^2(\omega) - 1 + (1 + 8v^2(\omega))^{3/2} \right]. \quad (5)$$

It should be noted that $v(\omega) = 1$ for $\mu = 0$ and from Eqs. (3)-(5) we recover the existence of the so-called black hole photon sphere located at $r_c(\omega) = 3M$ (the place on which the massless particles can orbit the black hole on unstable circular null geodesics). Moreover, in this case, the corresponding critical impact parameter is given by $b_c(\omega) = 3\sqrt{3}M$ and, as a consequence, the geometrical cross section $\sigma_{\text{geo}}(\omega) = 27\pi M^2$ of this black hole for massless particles is also recovered. It should be also noted that for $\mu \neq 0$ we have the asymptotic expansions

$$r_c(\omega) = 3M \left[1 + \frac{\mu^2}{9\omega^2} + \mathcal{O}_{\omega \rightarrow +\infty} \left(\frac{1}{\omega^4} \right) \right], \quad (6a)$$

$$b_c(\omega) = 3\sqrt{3}M \left[1 + \frac{\mu^2}{3\omega^2} + \mathcal{O}_{\omega \rightarrow +\infty} \left(\frac{1}{\omega^4} \right) \right], \quad (6b)$$

$$\sigma_{\text{geo}}(\omega) = 27\pi M^2 \left[1 + \frac{2\mu^2}{3\omega^2} + \mathcal{O}_{\omega \rightarrow +\infty} \left(\frac{1}{\omega^4} \right) \right]. \quad (6c)$$

So, at high energy, a massive particle behaves as a massless one and, in particular, orbits the black hole on unstable circular geodesics very near the photon sphere.

From now on, we consider a massive scalar field Φ with mass μ propagating on the exterior of the Schwarzschild black hole. It satisfies the wave equation $(\square - \mu^2)\Phi = 0$ which reduces, after separation of variables and the introduction of the radial partial wave functions $\phi_{\omega,\ell}(r)$ with $\omega > 0$ and $\ell \in \mathbb{N}$, to the Regge-Wheeler equation

$$\frac{d^2 \phi_{\omega,\ell}}{dr_*^2} + [\omega^2 - V_\ell(r)] \phi_{\omega,\ell} = 0. \quad (7)$$

In Eq. (7), $V_\ell(r)$ denotes the Regge-Wheeler potential given by

$$V_\ell(r) = \left(1 - \frac{2M}{r}\right) \left[\mu^2 + \frac{(\ell + 1/2)^2 - 1/4}{r^2} + \frac{2M}{r^3} \right] \quad (8)$$

while r_* is the so-called tortoise coordinate defined from the radial Schwarzschild coordinate r by $dr/dr_* = (1 - 2M/r)$. Here, it is important to recall that the function $r_* = r_*(r)$ provides a bijection from $]2M, +\infty[$ to $]-\infty, +\infty[$.

In this paper, we shall focus on the *IN*-modes (see, e.g., Ref. [58] or Chap. 30 of Ref. [59]) which are the solutions of (7) with a purely ingoing behavior at the event horizon $r = 2M$, i.e., which satisfy

$$\phi_{\omega,\ell}(r) \underset{r_* \rightarrow -\infty}{\sim} T_\ell(\omega) e^{-i\omega r_*} \quad (9a)$$

and which furthermore, at spatial infinity $r \rightarrow +\infty$, have an asymptotic behavior of the form

$$\begin{aligned} \phi_{\omega,\ell}(r) \underset{r_* \rightarrow +\infty}{\sim} & \left[\frac{\omega}{p(\omega)} \right]^{1/2} \\ & \times \left(e^{-i[p(\omega)r_* + (M\mu^2/p(\omega)) \ln(r/M)]} \right. \\ & \left. + R_\ell(\omega) e^{+i[p(\omega)r_* + (M\mu^2/p(\omega)) \ln(r/M)]} \right). \end{aligned} \quad (9b)$$

In Eq. (9b), $p(\omega)$ which now denotes the “wave number” is given by

$$p(\omega) = (\omega^2 - \mu^2)^{1/2} \quad (10)$$

while $T_\ell(\omega)$ and $R_\ell(\omega)$ are transmission and reflection coefficients linked by

$$|R_\ell(\omega)|^2 + |T_\ell(\omega)|^2 = 1 \quad \forall \omega > 0 \text{ and } \forall \ell \in \mathbb{N}. \quad (11)$$

It is interesting to note that this relation can be derived from the properties of the Wronskian

$$\begin{aligned} W[\phi_{\omega,\ell}(r), \overline{\phi_{\omega,\ell}(r)}] & \equiv \phi_{\omega,\ell}(r) \left(\frac{d}{dr_*} \overline{\phi_{\omega,\ell}(r)} \right) \\ & - \left(\frac{d}{dr_*} \phi_{\omega,\ell}(r) \right) \overline{\phi_{\omega,\ell}(r)}. \end{aligned} \quad (12)$$

Indeed, from (7) we can show that this Wronskian is a constant and by evaluating it for $r_* \rightarrow -\infty$ and for $r_* \rightarrow +\infty$ taking into account the boundary conditions

(9), we then obtain relation (11). It should be also noted that the coefficient $[\omega/p(\omega)]^{1/2}$ in Eq. (9b) has been introduced in order to simplify the form of this relation. It is moreover important to remark that the *IN*-modes are naturally and without any ambiguity defined by the boundary conditions (9) for $\omega > \mu$. However, for $0 < \omega < \mu$, the situation is a little bit more complicated (see Chap. 30 of Ref. [59] for more precisions): indeed, it is first necessary to go into the complex ω plane and to carefully take into account the various branch cuts associated with the functions $p(\omega)$ (the two cuts $]-\infty, -\mu[$ and $] +\mu, +\infty[$ along the real ω axis) and $\omega^{1/2}$ (e.g., a cut emanating from the origin and along the negative imaginary ω axis) allowing us to deal with these multi-valued functions; then, by working on the Riemann sheet in which $\text{Im } p(\omega) \geq 0$ (the first Riemann sheet in the following), we can define $p(\omega)$ for $0 < \omega < \mu$ and we have in particular $p(\omega)$ which is a pure positive imaginary; and, finally, the boundary conditions (9) can now be used even for $0 < \omega < \mu$.

Moreover, it is worth recalling that the transmission coefficients $T_\ell(\omega)$ permit us to construct the greybody factors (the absorption probabilities by the Schwarzschild black hole for scalar particles with energy ω and angular momentum ℓ). They are given by

$$\Gamma_\ell(\omega) = |T_\ell(\omega)|^2 \quad (13)$$

and, for the massive scalar field considered here, the black hole absorption cross section can be expressed in terms of them in the form

$$\sigma_{\text{abs}}(\omega) = \frac{\pi}{[p(\omega)]^2} \sum_{\ell=0}^{+\infty} (2\ell + 1) \Gamma_\ell(\omega). \quad (14)$$

Furthermore, even if we do not intend to analyze all the aspects of scattering by this black hole and to consider in particular its partial elastic cross sections, its scattering amplitude, its differential cross section, etc. ..., it is interesting to recall that all these concepts are built from the *S*-matrix which is defined by its diagonal elements

$$S_\ell(\omega) = (-1)^{\ell+1} R_\ell(\omega). \quad (15)$$

Finally, it should be noted that the *IN*-modes alone do not permit us to construct a basis of the solutions of the wave equation but they are sufficient in order to describe the resonance and absorption spectra of the Schwarzschild black hole. In other words, here it is not necessary to consider the usual *UP*-modes or to work with the alternative *OUT*- and *DOWN*-modes (see, e.g., Chap. 4 of Ref. [60] or Chap. 30 of Ref. [59]).

Let us now consider the Regge-Wheeler potential $V_\ell(r)$ given by (8). From now on, we shall assume that the condition

$$2M\mu \in]0, 1/2[\quad (16)$$

is satisfied. We shall therefore restrict our study to scalar field mass μ rather weak. This assumption allows us

to simplify our study because it saves us from complicated discussions on the behavior of $V_\ell(r)$ for different values of the angular momentum ℓ . Indeed, it is well-known [26, 43] that under (16), $V_\ell(r)$ always presents three extrema $\forall \ell \in \mathbb{N}$. Thanks to Tartaglia and Cardano, it is furthermore easy to prove that these extrema $r_{\text{neg}}(\ell)$, $r_{\text{max}}(\ell)$ and $r_{\text{min}}(\ell)$ satisfy $r_{\text{neg}}(\ell) < 0 < 8M/3 \leq r_{\text{max}}(\ell) < 4M < r_{\text{min}}(\ell)$ and are given by

$$r_{\text{neg}}(\ell) = \frac{\ell(\ell+1)}{3M\mu^2} + 2\sqrt{-\frac{\mathcal{P}(\ell)}{3}} \cos\left[\frac{\xi(\ell)}{3} + \frac{2\pi}{3}\right], \quad (17a)$$

$$r_{\text{max}}(\ell) = \frac{\ell(\ell+1)}{3M\mu^2} + 2\sqrt{-\frac{\mathcal{P}(\ell)}{3}} \cos\left[\frac{\xi(\ell)}{3} - \frac{2\pi}{3}\right], \quad (17b)$$

$$r_{\text{min}}(\ell) = \frac{\ell(\ell+1)}{3M\mu^2} + 2\sqrt{-\frac{\mathcal{P}(\ell)}{3}} \cos\left[\frac{\xi(\ell)}{3}\right], \quad (17c)$$

where

$$\mathcal{P}(\ell) = \frac{-1}{3M^2\mu^4} [\ell^2(\ell+1)^2 - 9M^2\mu^2\ell(\ell+1) + 9M^2\mu^2] \quad (18a)$$

and

$$\xi(\ell) = \arccos\left[-\frac{\mathcal{Q}(\ell)}{2} \sqrt{-\frac{27}{\mathcal{P}(\ell)^3}}\right] \quad (18b)$$

with

$$\mathcal{Q}(\ell) = \frac{-1}{27M^3\mu^6} [2\ell^3(\ell+1)^3 - 27M^2\mu^2\ell^2(\ell+1)^2 + 27M^2\mu^2\ell(\ell+1) - 216M^4\mu^4]. \quad (18c)$$

[For $\ell = 0$, (17) agrees with Eq. (13) of Ref. [43].] Of course, only the extrema $r_{\text{max}}(\ell)$ and $r_{\text{min}}(\ell)$ which lie in the physical region $r > 2M$ govern the behavior of the *IN*-modes defined above by the Regge-Wheeler equation (7) and the boundary conditions (9) and, furthermore, it is very important to keep in mind that $r_{\text{max}}(\ell)$ corresponds to the peak of a local potential barrier while $r_{\text{min}}(\ell)$ denotes the minimum of a local potential well. Finally, it is interesting to note that

$$r_{\text{max}}(\ell) = 3M \left[1 - \frac{1 - 27M^2\mu^2}{9(\ell + 1/2)^2} + \mathcal{O}_{\ell+1/2 \rightarrow +\infty} \left(\frac{1}{(\ell + 1/2)^4} \right) \right] \quad (19)$$

and therefore, for large angular momenta, the peak of the Regge-Wheeler potential $V_\ell(r)$ lies very near the photon sphere of the Schwarzschild black hole located at $r = 3M$.

The process which has allowed us to define the *IN*-modes for $0 < \omega < \mu$ moreover permits us to extend for complex ω values the diagonal matrices T , R and S . We recall that a pole of $T_\ell(\omega)$ [let us note that it is also a pole of $R_\ell(\omega)$ and $S_\ell(\omega)$] such that $T_\ell(\omega)/R_\ell(\omega)$ remains regular and which lies in the lower half plane of the first

Riemann sheet associated with the multivalued function $p(\omega)$ is a resonance of the scalar field. We also recall that resonances are symmetrically distributed with respect to the imaginary ω axis. We shall focus our attention on those lying in the fourth quadrant of the considered Riemann sheet. It is well-known that they can be separated into two families (see, e.g., Chap. 30 of Ref. [59] or Refs. [16, 20, 23, 25, 26, 36, 43]) corresponding respectively to complex frequencies ω satisfying $\text{Re}\omega < \mu$ and $\text{Re}\omega > \mu$ and therefore respectively associated with [see Eq. (9)]:

- a bound state spectrum (these modes are normalizable, purely ingoing at the horizon and fall off exponentially at spatial infinity),

- a quasinormal mode spectrum (these modes are not normalizable, purely ingoing at the horizon and purely outgoing at spatial infinity and they oscillate at both boundaries).

From a physical point of view, the existence of the bound state spectrum is directly related to the presence of the potential well close to $r_{\text{min}}(\ell)$ (see also Refs. [16, 20, 23, 25, 43] and Chap. 30 of Ref. [59] for more precisions) while the existence of the weakly damped quasinormal modes is due to the presence of the potential barrier at $r_{\text{max}}(\ell)$ or, equivalently, can be semiclassically described in terms of “surface waves” lying close to the photon sphere at $r = 3M$. In the remaining of this section, we intend to discuss more precisely this last point by using the CAM machinery. We are not able to provide an analogous description for the bound state spectrum.

To conclude this subsection, we shall briefly recall some aspects of CAM techniques we shall extensively use in the following. We first note that, for $\omega > 0$, the matrices T , R and S previously defined can be analytically extended into the CAM plane: we transform the ordinary angular momentum ℓ into a complex number $\lambda = \ell + 1/2$ and we construct the analytic extensions $T_{\lambda-1/2}(\omega)$, $R_{\lambda-1/2}(\omega)$ and $S_{\lambda-1/2}(\omega)$ of $T_\ell(\omega)$, $R_\ell(\omega)$ and $S_\ell(\omega)$ from (7), (8), (9) and (15). Let us also recall that the Regge poles are defined as the poles of the T -matrix [or, equivalently, as the poles of the matrices R or S] for which $T_{\lambda-1/2}(\omega)/R_{\lambda-1/2}(\omega)$ remains regular and that they lie in the first and third quadrants of the CAM plane symmetrically distributed with respect to its origin. The Regge poles can be also considered as “eigenvalues” associated with the so-called Regge modes $\phi_{\omega, \lambda-1/2}(r)$ which satisfy (7) and are purely ingoing at the horizon and purely outgoing at spatial infinity [see Eq. (9)]. In Ref. [48] we showed that, for a massless scalar field propagating on the Schwarzschild black hole, the complex frequencies of the weakly damped quasinormal modes can be obtained analytically from the so-called Regge trajectories, i.e., from the curves traced out in the CAM plane by the Regge poles as a function of the frequency ω . *Mutatis mutandis*, the reasoning leading to these results (see for more precisions Refs. [45, 48] and Appendix A of Ref. [49]) can be repeated in the context of a massive scalar field theory. Let us denote by

$\omega_{\ell n} = \omega_{\ell n}^{(o)} - i\Gamma_{\ell n}/2$ with $\ell \in \mathbb{N}$ and $n \in \mathbb{N} \setminus \{0\}$ the complex quasinormal frequencies lying in the lower half plane of the first Riemann sheet associated with the multivalued function $p(\omega)$ and by λ_n with $n \in \mathbb{N} \setminus \{0\}$ the Regge poles lying in the first quadrant of the CAM plane. If we describe the associated Regge trajectories by the functions $\lambda_n = \lambda_n(\omega)$ with $\omega > \mu$, we have the semiclassical relations

$$\text{Re } \lambda_n \left(\omega_{\ell n}^{(o)} \right) = \ell + 1/2 \quad \ell \in \mathbb{N}, \quad (20a)$$

and

$$\frac{\Gamma_{\ell n}}{2} = \left. \frac{\text{Im } \lambda_n(\omega)}{d/d\omega \text{ Re } \lambda_n(\omega)} \right|_{\omega=\omega_{\ell n}^{(o)}}. \quad (20b)$$

B. Regge poles: The Dolan-Ottewill method

In this subsection, we shall obtain high-frequency asymptotic expansions for the Regge poles by using and extending to the massive scalar field a new and powerful method introduced and developed by Dolan and Ottewill in Ref. [47]. It is important to note (see below) that, in this method, the critical parameters (3) and (4) associated with the massive scalar particle are the main ingredients permitting us to construct the Regge modes and the Regge poles associated with the field theory.

Extending the reasoning of Dolan and Ottewill to the massive scalar field, we introduce the following ansatz to describe the Regge modes $\phi_{\omega, \lambda_n(\omega)-1/2}(r)$ and the corresponding Regge poles $\lambda_n(\omega)$:

$$\phi_{\omega, \lambda_n(\omega)-1/2}(r) = u_{\omega, \lambda_n(\omega)-1/2}(r) \exp \left[i\omega v(\omega) \int^{r_*} \left(1 + \frac{2Mb_c(\omega)^2/r_c(\omega)^2}{r'} \right)^{\frac{1}{2}} \left(1 - \frac{r_c(\omega)}{r'} \right) dr'_* \right] \quad (21a)$$

with

$$u_{\omega, \lambda_n(\omega)-1/2}(r) = \left[\left(1 - \frac{r_c(\omega)}{r} \right)^n + \sum_{i=1}^n \sum_{j=1}^{\infty} b_{ij}^{(n)}(\omega) [\omega v(\omega)]^{-j} \left(1 - \frac{r_c(\omega)}{r} \right)^{n-i} \right] \exp \left(\sum_{k=0}^{\infty} T_k^{(n)}(\omega, r) [\omega v(\omega)]^{-k} \right) \quad (21b)$$

and

$$\lambda_n(\omega) = \lambda_{-1}^{(n)}(\omega v(\omega)) [\omega v(\omega)] + \lambda_0^{(n)}(\omega v(\omega)) + \frac{\lambda_1^{(n)}(\omega v(\omega))}{[\omega v(\omega)]} + \frac{\lambda_2^{(n)}(\omega v(\omega))}{[\omega v(\omega)]^2} + \frac{\lambda_3^{(n)}(\omega v(\omega))}{[\omega v(\omega)]^3} + \frac{\lambda_4^{(n)}(\omega v(\omega))}{[\omega v(\omega)]^4} + \dots \quad (22)$$

We invite the reader to compare our Eqs. (21a), (21b) and (22) with Eqs. (5), (39) and (38) of Ref. [47]. It should be noted more particularly that, in order to extend the Dolan-Ottewill method for the massive scalar field, we must consider as the natural asymptotic parameter the ‘‘momentum’’ $\omega v(\omega) = p(\omega)$ instead of the energy ω and assume that $\omega > \mu$.

By inserting Eqs. (21a), (21b) and (22) into (7) with (8) where $\ell \rightarrow \lambda_n(\omega) - 1/2$ and after a tedious calculation, we obtain

$$\lambda_{-1}^{(n)}(\omega v(\omega)) = 3\sqrt{3}M \left[1 + \frac{1}{3} \left(\frac{\mu^2}{[\omega v(\omega)]^2} \right) - \frac{2}{27} \left(\frac{\mu^4}{[\omega v(\omega)]^4} \right) + \mathcal{O}_{\mu/[\omega v(\omega)] \rightarrow 0} \left(\frac{\mu^6}{[\omega v(\omega)]^6} \right) \right], \quad (23a)$$

$$\lambda_0^{(n)}(\omega v(\omega)) = i\alpha(n) \left[1 - \frac{1}{9} \left(\frac{\mu^2}{[\omega v(\omega)]^2} \right) + \frac{1}{18} \left(\frac{\mu^4}{[\omega v(\omega)]^4} \right) + \mathcal{O}_{\mu/[\omega v(\omega)] \rightarrow 0} \left(\frac{\mu^6}{[\omega v(\omega)]^6} \right) \right], \quad (23b)$$

$$\lambda_1^{(n)}(\omega v(\omega)) = \frac{3\sqrt{3}}{M} \left[\frac{60\alpha(n)^2 - 29}{11664} + \frac{-372\alpha(n)^2 + 115}{104976} \left(\frac{\mu^2}{[\omega v(\omega)]^2} \right) + \mathcal{O}_{\mu/[\omega v(\omega)] \rightarrow 0} \left(\frac{\mu^4}{[\omega v(\omega)]^4} \right) \right], \quad (23c)$$

$$\lambda_2^{(n)}(\omega v(\omega)) = i \frac{\alpha(n)}{M^2} \left[\frac{-1220\alpha(n)^2 + 1357}{419904} + \frac{4444\alpha(n)^2 - 3707}{1259712} \left(\frac{\mu^2}{[\omega v(\omega)]^2} \right) + \mathcal{O}_{\mu/[\omega v(\omega)] \rightarrow 0} \left(\frac{\mu^4}{[\omega v(\omega)]^4} \right) \right], \quad (23d)$$

$$\lambda_3^{(n)}(\omega v(\omega)) = \frac{3\sqrt{3}}{M^3} \left[\frac{-2357520\alpha(n)^4 + 4630008\alpha(n)^2 - 99373}{29386561536} + \mathcal{O}_{\mu/[\omega v(\omega)] \rightarrow 0} \left(\frac{\mu^2}{[\omega v(\omega)]^2} \right) \right], \quad (23e)$$

$$\lambda_4^{(n)}(\omega v(\omega)) = i \frac{\alpha(n)}{M^4} \left[\frac{144920784\alpha(n)^4 - 439855800\alpha(n)^2 + 28395953}{2115832430592} + \mathcal{O}_{\mu/[\omega v(\omega)] \rightarrow 0} \left(\frac{\mu^2}{[\omega v(\omega)]^2} \right) \right], \quad (23f)$$

and finally

$$\begin{aligned}
\lambda_n(\omega) = & 3\sqrt{3}M\omega v(\omega) + i\alpha(n) + \left[\frac{5}{36}\alpha(n)^2 - \frac{29 - 3888M^2\mu^2}{432} \right] \left(\frac{1}{(3\sqrt{3}M\omega v(\omega))} \right) \\
& + i\alpha(n) \left[-\frac{305}{3888}\alpha(n)^2 + \frac{1357 - 46656M^2\mu^2}{15552} \right] \left(\frac{1}{(3\sqrt{3}M\omega v(\omega))^2} \right) \\
& + \left[-\frac{49115}{839808}\alpha(n)^4 + \frac{192917 - 4339008M^2\mu^2}{1679616}\alpha(n)^2 \right. \\
& \quad \left. - \frac{99373 - 32192640M^2\mu^2 + 2176782336M^4\mu^4}{40310784} \right] \left(\frac{1}{(3\sqrt{3}M\omega v(\omega))^3} \right) \\
& + i\alpha(n) \left[\frac{3019183}{60466176}\alpha(n)^4 - \frac{18327325 - 311008896M^2\mu^2}{120932352}\alpha(n)^2 \right. \\
& \quad \left. + \frac{28395953 - 6226336512M^2\mu^2 + 117546246144M^4\mu^4}{2902376448} \right] \left(\frac{1}{(3\sqrt{3}M\omega v(\omega))^4} \right) \\
& + \mathcal{O}_{M\omega v(\omega) \rightarrow +\infty} \left(\frac{1}{(3\sqrt{3}M\omega v(\omega))^5} \right). \tag{24}
\end{aligned}$$

In the previous equations, we have

$$\alpha(n) = n - 1/2 \quad \text{for } n \in \mathbb{N} \setminus \{0\}. \tag{25}$$

We can also convert the previous asymptotic expansion in $\omega v(\omega)$ into an asymptotic expansion in ω . From (2) or (10), we have

$$\begin{aligned}
\lambda_n(\omega) = & 3\sqrt{3}M\omega + i\alpha(n) + \left[\frac{5}{36}\alpha(n)^2 - \frac{29 + 1944M^2\mu^2}{432} \right] \left(\frac{1}{(3\sqrt{3}M\omega)} \right) \\
& + i\alpha(n) \left[-\frac{305}{3888}\alpha(n)^2 + \frac{1357 - 46656M^2\mu^2}{15552} \right] \left(\frac{1}{(3\sqrt{3}M\omega)^2} \right) \\
& + \left[-\frac{49115}{839808}\alpha(n)^4 + \frac{192917 - 1189728M^2\mu^2}{1679616}\alpha(n)^2 - \frac{99373 + 4339008M^2\mu^2 + 952342272M^4\mu^4}{40310784} \right] \left(\frac{1}{(3\sqrt{3}M\omega)^3} \right) \\
& + i\alpha(n) \left[\frac{3019183}{60466176}\alpha(n)^4 - \frac{18327325 - 54867456M^2\mu^2}{120932352}\alpha(n)^2 \right. \\
& \quad \left. + \frac{28395953 + 611380224M^2\mu^2 - 117546246144M^4\mu^4}{2902376448} \right] \left(\frac{1}{(3\sqrt{3}M\omega)^4} \right) + \mathcal{O}_{M\omega \rightarrow +\infty} \left(\frac{1}{(3\sqrt{3}M\omega)^5} \right). \tag{26}
\end{aligned}$$

For $\mu = 0$, formula (26) is in agreement with Eq. (38) and Eqs. (40)-(45) of Ref. [47].

C. Regge poles: The WKB approach

In this subsection, we shall derive again the high-frequency asymptotic expansion (26) for the Regge poles but, now, we shall use a more traditional approach (see Refs. [48, 49] for previous applications to massless theories) based on the WKB method developed a long time ago by Schutz, Will and Iyer [51–54] (and extended to higher orders by Konoplya [55]) to study the resonant behavior of black holes and to determine more particularly their weakly damped quasinormal frequencies. We shall thus check formula (26) but we shall also see that

the Dolan-Ottewill method is, in the context of the Regge pole determination, a much more powerful approach than the WKB one providing more quickly the same results when we need to capture higher-order terms in asymptotic expansions. Indeed, in order to derive (26) we shall now start with a fifth-order WKB approximation for the greybody factors (13) and, therefore, we shall work with very heavy expressions (see below). Of course, if we only need the leading order or the next-to-leading order of the asymptotic expansion (26), it seems to us that the WKB approach remains more tractable.

Before to begin the technical part of our work, it is also interesting to note that the Dolan-Ottewill method developed in the previous subsection and the WKB approach we shall use here are based on different physical concepts. Indeed, as already previously noted, the Dolan-Ottewill

ansatz is constructed from the critical parameters (3) and (4) associated with the massive particle while the WKB calculation will extensively use the maximum (17b) of the Regge-Wheeler potential defining the scalar field theory. Of course, in both approaches, for very high frequencies, it is the photon sphere at $r_c(\omega) = 3M$ and the corresponding impact parameter $b_c(\omega) = 3\sqrt{3}M$ which play the crucial role.

For $\ell \in \mathbb{N}$ and $\omega > 0$ with ω^2 near the peak $V_\ell(r_{\max}(\ell))$ of the Regge-Wheeler potential, we can use, following

Iyer, Will and Guinn [52–54] and taking into account some results displayed in Ref. [55], a fifth-order WKB approximation for the greybody factors (13). After a tedious calculation, we obtain

$$\Gamma_\ell(\omega) = \frac{1}{1 + \exp[2\mathcal{S}_\ell(\omega)]} \quad (27)$$

with

$$\begin{aligned} \mathcal{S}_\ell(\omega) = & \pi k^{1/2} \left\{ \frac{1}{2} z_0^2 + \left(\frac{15}{64} b_3^2 - \frac{3}{16} b_4 \right) z_0^4 + \left(\frac{1155}{2048} b_3^4 - \frac{315}{256} b_3^2 b_4 + \frac{35}{64} b_3 b_5 + \frac{35}{128} b_4^2 - \frac{5}{32} b_6 \right) z_0^6 \right. \\ & + \left(\frac{255255}{131072} b_3^6 - \frac{225225}{32768} b_3^4 b_4 + \frac{15015}{4096} b_3^3 b_5 + \frac{45045}{8192} b_3^2 b_4^2 - \frac{3465}{2048} b_3^2 b_6 - \frac{3465}{1024} b_3 b_4 b_5 + \frac{315}{512} b_3 b_7 \right. \\ & - \frac{1155}{2048} b_4^3 + \frac{315}{512} b_4 b_6 + \frac{315}{1024} b_5^2 - \frac{35}{256} b_8 \left. \right) z_0^8 + \left(\frac{66927861}{8388608} b_3^8 - \frac{20369349}{524288} b_3^6 b_4 + \frac{2909907}{131072} b_3^5 b_5 \right. \\ & + \frac{14549535}{262144} b_3^4 b_4^2 - \frac{765765}{65536} b_3^4 b_6 - \frac{765765}{16384} b_3^3 b_4 b_5 + \frac{45045}{8192} b_3^3 b_7 - \frac{765765}{32768} b_3^2 b_4^3 + \frac{135135}{8192} b_3^2 b_4 b_6 \\ & + \frac{135135}{16384} b_3^2 b_5^2 - \frac{9009}{4096} b_3^2 b_8 + \frac{135135}{8192} b_3 b_4^2 b_5 - \frac{9009}{2048} b_3 b_4 b_7 - \frac{9009}{2048} b_3 b_5 b_6 + \frac{693}{1024} b_3 b_9 + \frac{45045}{32768} b_4^4 \\ & - \frac{9009}{4096} b_4^2 b_6 - \frac{9009}{4096} b_4 b_5^2 + \frac{693}{1024} b_4 b_8 + \frac{693}{1024} b_5 b_7 + \frac{693}{2048} b_6^2 - \frac{63}{512} b_{10} \left. \right) z_0^{10} \left. \right\} \\ & + \pi k^{-1/2} \left\{ \left(-\frac{7}{64} b_3^2 + \frac{3}{16} b_4 \right) + \left(-\frac{1365}{2048} b_3^4 + \frac{525}{256} b_3^2 b_4 - \frac{95}{64} b_3 b_5 - \frac{85}{128} b_4^2 + \frac{25}{32} b_6 \right) z_0^2 \right. \\ & + \left(-\frac{285285}{65536} b_3^6 + \frac{315315}{16384} b_3^4 b_4 - \frac{28875}{2048} b_3^3 b_5 - \frac{79695}{4096} b_3^2 b_4^2 + \frac{9765}{1024} b_3^2 b_6 + \frac{8505}{512} b_3 b_4 b_5 - \frac{1365}{256} b_3 b_7 \right. \\ & + \frac{2625}{1024} b_4^3 - \frac{1155}{256} b_4 b_6 - \frac{1085}{512} b_5^2 + \frac{245}{128} b_8 \left. \right) z_0^4 + \left(-\frac{121246125}{4194304} b_3^8 + \frac{43648605}{262144} b_3^6 b_4 - \frac{7912905}{65536} b_3^5 b_5 \right. \\ & - \frac{37011975}{131072} b_3^4 b_4^2 + \frac{2777775}{32768} b_3^4 b_6 + \frac{2477475}{8192} b_3^3 b_4 b_5 - \frac{225225}{4096} b_3^3 b_7 + \frac{2327325}{16384} b_3^2 b_4^3 - \frac{585585}{4096} b_3^2 b_4 b_6 \\ & - \frac{555555}{8192} b_3^2 b_5^2 + \frac{63525}{2048} b_3^2 b_8 - \frac{525525}{4096} b_3 b_4^2 b_5 + \frac{54285}{1024} b_3 b_4 b_7 + \frac{49665}{1024} b_3 b_5 b_6 - \frac{7035}{512} b_3 b_9 - \frac{165165}{16384} b_4^4 \\ & + \frac{47355}{2048} b_4^2 b_6 + \frac{45045}{2048} b_4 b_5^2 - \frac{5985}{512} b_4 b_8 - \frac{5355}{512} b_5 b_7 - \frac{5145}{1024} b_6^2 + \frac{945}{256} b_{10} \left. \right) z_0^6 \left. \right\} \\ & + \pi k^{-3/2} \left\{ \left(\frac{119119}{131072} b_3^6 - \frac{153153}{32768} b_3^4 b_4 + \frac{16107}{4096} b_3^3 b_5 + \frac{47229}{8192} b_3^2 b_4^2 - \frac{6405}{2048} b_3^2 b_6 - \frac{6237}{1024} b_3 b_4 b_5 + \frac{1155}{512} b_3 b_7 \right. \right. \\ & - \frac{1995}{2048} b_4^3 + \frac{1095}{512} b_4 b_6 + \frac{1107}{1024} b_5^2 - \frac{315}{256} b_8 \left. \right) + \left(\frac{156165009}{8388608} b_3^8 - \frac{63864801}{524288} b_3^6 b_4 + \frac{13216203}{131072} b_3^5 b_5 \right. \\ & + \frac{62777715}{262144} b_3^4 b_4^2 - \frac{5354349}{65536} b_3^4 b_6 - \frac{4945941}{16384} b_3^3 b_4 b_5 + \frac{519057}{8192} b_3^3 b_7 - \frac{4669665}{32768} b_3^2 b_4^3 + \frac{1399167}{8192} b_3^2 b_4 b_6 \\ & + \frac{1368675}{16384} b_3^2 b_5^2 - \frac{185661}{4096} b_3^2 b_8 + \frac{1279047}{8192} b_3 b_4^2 b_5 - \frac{161133}{2048} b_3 b_4 b_7 - \frac{154917}{2048} b_3 b_5 b_6 + \frac{28077}{1024} b_3 b_9 \\ & \left. \left. + \frac{400785}{32768} b_4^4 - \frac{143241}{4096} b_4^2 b_6 - \frac{139293}{4096} b_4 b_5^2 + \frac{23457}{1024} b_4 b_8 + \frac{22029}{1024} b_5 b_7 + \frac{21777}{2048} b_6^2 - \frac{5607}{512} b_{10} \right) z_0^8 \right\}. \quad (28) \end{aligned}$$

Here, we use the notations

$$z_0 \equiv z_0(\ell, \omega) = \sqrt{2 \frac{\omega^2 - V_0(\ell)}{V_0^{(2)}(\ell)}}, \quad (29)$$

$$k \equiv k(\ell) = -\frac{1}{2} V_0^{(2)}(\ell), \quad (30)$$

and

$$b_p \equiv b_p(\ell) = \frac{2}{p!} \frac{V_0^{(p)}(\ell)}{V_0^{(2)}(\ell)} \quad \text{for } p > 2, \quad (31)$$

with

$$V_0(\ell) \equiv V_\ell(r_*)|_{r_*=r_*[r_{\max}(\ell)]} = V_\ell(r)|_{r=r_{\max}(\ell)} \quad (32)$$

and

$$V_0^{(p)}(\ell) \equiv \left. \frac{d^p}{dr_*^p} V_\ell(r_*) \right|_{r_*=r_*[r_{\max}(\ell)]} \quad \text{for } p \geq 2. \quad (33)$$

It should be noted that, in Eq. (28), the term $k^{1/2}z_0^2$ corresponds to the first-order WKB approximation. Adding the terms $k^{1/2}z_0^4$ and $k^{-1/2}$ permits us to construct the second-order WKB approximation. Adding furthermore the terms $k^{1/2}z_0^6$ and $k^{-1/2}z_0^2$ permits us to obtain the third-order WKB approximation. Finally, adding the terms $k^{1/2}z_0^8$, $k^{-1/2}z_0^4$ and $k^{-3/2}$ provides us with the fourth-order WKB approximation. This fourth-order WKB approximation can be found in Ref. [54] (see Eq. (12) of that paper) and is confirmed by our own calculations, even if some coefficients in Eqs. (6) and (7) of Ref. [54] are wrong and if some misprints are present in Eq. (4). In Eq. (28) we have also taken into account the terms $k^{1/2}z_0^{10}$, $k^{-1/2}z_0^6$ and $k^{-3/2}z_0^2$ corresponding to the fifth-order WKB approximation. They have been obtained from Ref. [55]. It should be noted that we have been able to construct also the sixth-order WKB approximation of the greybody factors (27) by taking into account the terms $k^{1/2}z_0^{12}$, $k^{-1/2}z_0^8$, $k^{-3/2}z_0^4$ and $k^{-5/2}$.

Because we do not need it here, we do not display its very long expression but we can provide it upon request.

Even if formula (28) has been obtained for $\ell \in \mathbb{N}$ and $\omega > 0$, it can be used in the complex frequency plane or, as we intend to do here, in the complex angular momentum plane. We consider that $\omega > 0$ but we transform the angular momentum ℓ appearing in the previous equations into the complex variable $\lambda = \ell + 1/2$ and we then consider the analytic extension $\Gamma_{\lambda-1/2}(\omega)$ of the greybody factors $\Gamma_\ell(\omega)$ defined by (13) and (27) as well as the analytic extension $\mathcal{S}_{\lambda-1/2}(\omega)$ of the “phase” $\mathcal{S}_\ell(\omega)$ given by (28). We have

$$\Gamma_{\lambda-1/2}(\omega) = \frac{1}{1 + \exp[2\mathcal{S}_{\lambda-1/2}(\omega)]} \quad (34)$$

and the (Regge) poles of the greybody factors are the solutions $\lambda_n(\omega)$ of the equation

$$\mathcal{S}_{\lambda-1/2}(\omega) = i(n-1/2)\pi \quad \text{with } n \in \mathbb{N} \setminus \{0\} \quad (35)$$

(here we only consider those of the poles lying in the first quadrant of the CAM plane). By inserting (17b) into (28)-(33) and considering the transformation $\ell \rightarrow \lambda-1/2$, we obtain from (35)

$$\begin{aligned} (\omega M)^2 = & \left(\frac{1}{27}\right)\lambda^2 - i\left(\frac{2\alpha(n)}{27}\right)\lambda + \left[\left(\frac{29-276\alpha(n)^2}{5832}\right) + \frac{1}{3}M^2\mu^2\right] \\ & + i\left[\left(\frac{-1357\alpha(n)+1220\alpha(n)^3}{209952}\right) + \frac{2\alpha(n)}{9}M^2\mu^2\right]\left(\frac{1}{\lambda}\right) \\ & + \left[\left(\frac{8545-736824\alpha(n)^2-1193520\alpha(n)^4}{544195584}\right) + \left(\frac{-7-60\alpha(n)^2}{486}\right)M^2\mu^2 + M^4\mu^4\right]\left(\frac{1}{\lambda^2}\right) \\ & + i\left[\left(\frac{6835519\alpha(n)-20410824\alpha(n)^3-25861584\alpha(n)^5}{39182082048}\right) + \left(\frac{-125\alpha(n)-380\alpha(n)^3}{7776}\right)M^2\mu^2 + 3\alpha(n)M^4\mu^4\right]\left(\frac{1}{\lambda^3}\right) \\ & + \mathcal{O}_{\lambda \rightarrow +\infty}\left(\frac{1}{\lambda^4}\right). \end{aligned} \quad (36)$$

We can then solve (36) perturbatively to recover (26).

D. Regge poles: “Exact” versus asymptotic results

It is now interesting to check the accuracy of the high-frequency asymptotic expansions previously obtained. In Ref. [45], in order to determine numerically, for massless field theories, the Regge poles of the Schwarzschild black hole, we adapted the powerful method developed by Leaver [61] to calculate the complex quasinormal frequencies of the Schwarzschild and Kerr black holes (actually,

we implemented a slightly modified version of it due to Majumdar and Panchapakesan and based on the Hill determinant [62]). But, here, we are confronted with a massive scalar field and Leaver’s method must be modified. In Ref. [36], Konoplya and Zhidenko have shown how to achieve the corresponding modifications and, in this paper, we have combined the Leaver-Konoplya-Zhidenko method with the Hill determinant approach to deal numerically with the Regge pole spectrum.

Figure 1 exhibits the exact Regge trajectories numerically calculated and permits us to show clearly the role of the mass parameter μ . We also observe numerically

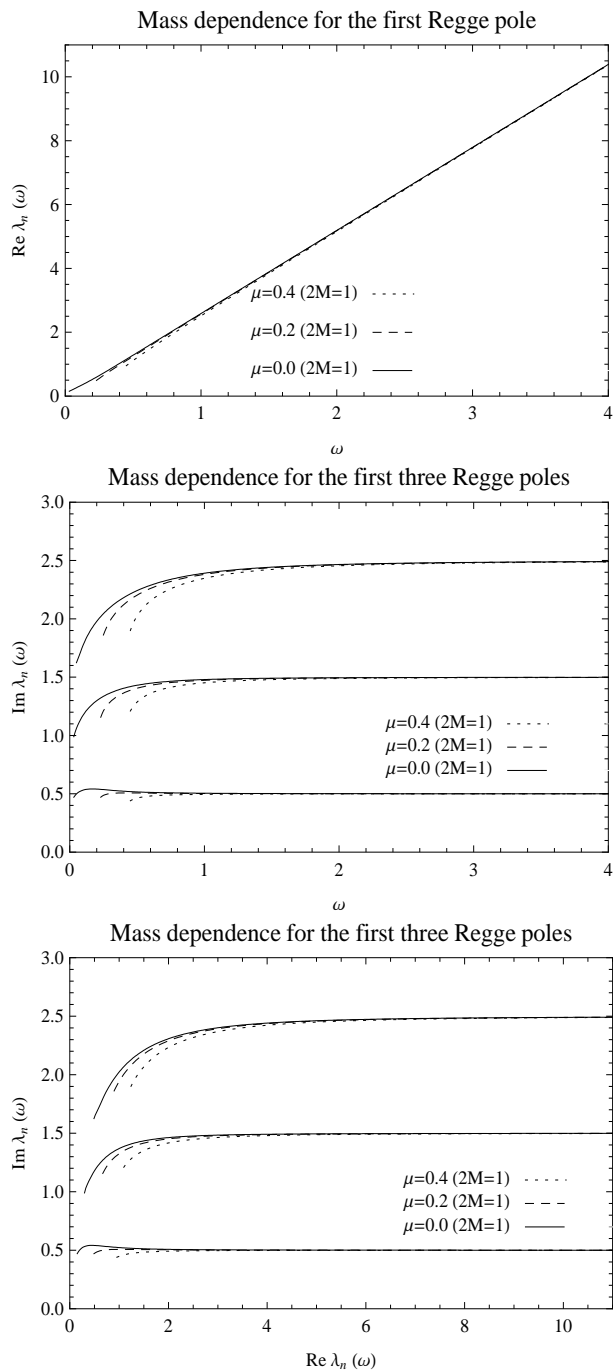


FIG. 1: Regge trajectories for the massless and the massive scalar fields (small masses satisfying (16)). The Regge poles $\lambda_n(\omega)$ ($n = 1, 2, 3$) are followed for $2M\omega = 0.03 \rightarrow 4$. For more readability, the plot of $\text{Re } \lambda_n(\omega)$ is displayed for the only first Regge pole.

that the Regge poles are only defined for $\omega > \mu$.

We have also compared the exact Regge poles numerically obtained with the results provided by the series (26) or by the series (24). The accuracy is very impressive for high frequencies (i.e. for $|2M\omega| \geq 2$) and the errors for both series are of the same order. However, it should be

TABLE I: A sample of Regge pole values for the scalar field: Exact versus asymptotic results for $\mu = 0$ ($2M = 1$). The series (24) is always truncated at the smallest term.

n	ω	Exact	Exact	Asymptotic	Asymptotic
		$\text{Re } \lambda_n(\omega)$	$\text{Im } \lambda_n(\omega)$	$\text{Re } \lambda_n(\omega)$	$\text{Im } \lambda_n(\omega)$
1	0.5	1.282821	0.515994	1.284398 (-0.12 %)	0.515656 (0.07 %)
	1.0	2.586845	0.504736	2.586891 (-0.0018 %)	0.504737 (-0.0002 %)
	2.0	5.190075	0.501236	5.190077 (-0.000039 %)	0.501236 (0. %)
2	0.5	1.452818	1.430687	1.469628 (-1.2 %)	1.379357 (3.6 %)
	1.0	2.688355	1.479587	2.690232 (-0.07 %)	1.477585 (0.14 %)
	2.0	5.242994	1.494926	5.243088 (-0.0018 %)	1.494880 (0.0031 %)

TABLE II: A sample of Regge pole values for the scalar field: Exact versus asymptotic results for $\mu = 0.2$ ($2M = 1$). The series (24) is always truncated at the smallest term.

n	ω	Exact	Exact	Asymptotic	Asymptotic
		$\text{Re } \lambda_n(\omega)$	$\text{Im } \lambda_n(\omega)$	$\text{Re } \lambda_n(\omega)$	$\text{Im } \lambda_n(\omega)$
1	0.5	1.245875	0.506823	1.250055 (-0.34 %)	0.504331 (0.49 %)
	1.0	2.569229	0.502503	2.569344 (-0.004 %)	0.502477 (0.005 %)
	2.0	5.181378	0.500679	5.181381 (-0.000066 %)	0.500679 (0. %)
2	0.5	1.411681	1.405188	1.4155982 (-0.3 %)	1.345471 (4.2 %)
	1.0	2.670066	1.473100	2.671532 (-0.055 %)	1.471040 (0.14 %)
	2.0	5.234201	1.493274	5.234282 (-0.0015 %)	1.493228 (0.0030 %)

noted that they increase slightly with the order of the Regge pole and with the magnitude of the mass parameter μ . For rather low frequencies, the series (24) is the most accurate one. Tables I-III present a sample of Regge pole positions calculated from this asymptotic formula. They exhibit a good agreement for the first Regge pole even for low frequencies. For the second Regge pole (and also for the third one not displayed here), the accuracy remains correct for $|2M\omega| \geq 1$.

E. Effect of the mass on the complex quasinormal frequencies

Formulas (20a) and (20b) permit us to construct analytical approximations for the resonance excitation frequencies $\omega_{\ell n}^{(0)}$ and the damping $\Gamma_{\ell n}/2$ of the quasinormal modes. By inserting into these two semiclassical formulas the series (26) truncated after the term in $1/(3\sqrt{3}M\omega)^2$,

TABLE III: A sample of Regge pole values for the scalar field: Exact versus asymptotic results for $\mu = 0.4$ ($2M = 1$). The series (24) is always truncated at the smallest term.

n	ω	Exact		Asymptotic	
		Re $\lambda_n(\omega)$	Im $\lambda_n(\omega)$	Re $\lambda_n(\omega)$	Im $\lambda_n(\omega)$
1	0.5	1.114489	0.462801	1.077877 (3.3 %)	0.429439 (7.2 %)
	1.0	2.514597	0.495198	2.514479 (0.005 %)	0.495068 (0.026 %)
	2.0	5.155079	0.498976	5.155077 (0.00004 %)	0.498975 (0.00020 %)
2	0.5	1.258631	1.286677	1.55611 (-24 %)	0.983336 (24 %)
	1.0	2.613157	1.451939	2.611183 (0.08 %)	1.450803 (0.08 %)
	2.0	5.207607	1.488218	5.207596 (0.00021 %)	1.488185 (0.00219 %)

we obtain

$$\begin{aligned} \omega_{\ell n}^{(0)} &= \frac{1}{3\sqrt{3}M} \left\{ (\ell + 1/2) \right. \\ &+ \left[-\frac{5}{36}\alpha(n)^2 + \frac{29 + 1944M^2\mu^2}{432} \right] \left(\frac{1}{(\ell + 1/2)} \right) \\ &+ \left. \mathcal{O}_{\ell \rightarrow +\infty} \left(\frac{1}{(\ell + 1/2)^3} \right) \right\}, \end{aligned} \quad (37a)$$

$$\begin{aligned} \frac{\Gamma_{\ell n}}{2} &= \frac{\alpha(n)}{3\sqrt{3}M} \left\{ 1 \right. \\ &+ \left[\frac{235}{3888}\alpha(n)^2 + \frac{313 - 116640M^2\mu^2}{15552} \right] \left(\frac{1}{(\ell + 1/2)^2} \right) \\ &+ \left. \mathcal{O}_{\ell \rightarrow +\infty} \left(\frac{1}{(\ell + 1/2)^4} \right) \right\}. \end{aligned} \quad (37b)$$

It should be noted that, for $\mu = 0$, formulas (37) are in agreement with the results obtained in Ref. [53] (see also Ref. [48]).

From Eq. (37), we can note that when the mass μ of the scalar field increases, the oscillation frequency of a quasinormal mode also increases while its damping decreases. This well-known result observed numerically by various authors (see, e.g., Refs. [26, 36]) is here analytically described. It is moreover possible to provide a dual explanation of this result by considering the physical interpretation of the Regge poles in terms of “surface waves” located close to the photon sphere [7, 45, 48, 49], even if we think that this description must taken with a grain of salt. In this context, we recall that $\text{Re } \lambda_n(\omega)$ represents the azimuthal propagation constant of the n -th surface wave while $\text{Im } \lambda_n(\omega)$ is its damping constant. From (26), it is then obvious that, for a fixed value of the frequency ω , all the azimuthal propagation constants and all the damping constants decrease when the mass parameter μ increases. As a consequence, the resonance excitation frequencies $\omega_{\ell n}^{(0)}$ which are the frequencies for which a constructive interference due to the surface waves occurs [see also Eq. (20a)] must necessarily increase with the mass parameter μ . Furthermore, because the attenuation of the n -th surface wave decreases when the mass parameter μ increases, the energy it radiates away during its repeated circumnavigations around the black hole also decreases; it is then natural [see also Eq. (20b)] to observe a similar behavior for the damping of the associated quasinormal modes.

We can greatly improve the asymptotic expansions (37) by going beyond the semiclassical approach. Indeed, the complex quasinormal frequencies are solutions of the equation

$$\lambda_n(\omega) = \ell + 1/2 \quad \text{with } n \in \mathbb{N} \setminus \{0\} \quad \text{and } \ell \in \mathbb{N}. \quad (38)$$

Such a result can be understood if we recall that a factor in $1/\cos[\pi\lambda_n(\omega)]$ appears in all the residues series over the Regge poles constructed from the CAM machinery (see, e.g., Eq. (8) of Ref. [45]). Equation (38) can be solved perturbatively and we then obtain

$$\begin{aligned} \omega_{\ell n}^{(0)} &= \frac{1}{3\sqrt{3}M} \left\{ (\ell + 1/2) + \left[-\frac{5}{36}\alpha(n)^2 + \frac{29 + 1944M^2\mu^2}{432} \right] \left(\frac{1}{(\ell + 1/2)} \right) \right. \\ &+ \left[\frac{17795}{839808}\alpha(n)^4 + \frac{18763 - 14346720M^2\mu^2}{1679616}\alpha(n)^2 - \frac{82283 + 20015424M^2\mu^2 - 136048896M^4\mu^4}{40310784} \right] \left(\frac{1}{(\ell + 1/2)^3} \right) \\ &+ \left. \mathcal{O}_{\ell \rightarrow +\infty} \left(\frac{1}{(\ell + 1/2)^5} \right) \right\}, \end{aligned} \quad (39a)$$

and

$$\begin{aligned} \frac{\Gamma_{\ell n}}{2} &= \frac{\alpha(n)}{3\sqrt{3}M} \left\{ 1 + \left[\frac{235}{3888}\alpha(n)^2 + \frac{313 - 116640M^2\mu^2}{15552} \right] \left(\frac{1}{(\ell + 1/2)^2} \right) \right. \\ &+ \left[-\frac{234857}{60466176}\alpha(n)^4 - \frac{653125 - 953881920M^2\mu^2}{120932352}\alpha(n)^2 \right. \\ &\quad \left. \left. - \frac{4832407 - 3269372544M^2\mu^2 + 29386561536M^4\mu^4}{2902376448} \right] \left(\frac{1}{(\ell + 1/2)^4} \right) + \mathcal{O}_{\ell \rightarrow +\infty} \left(\frac{1}{(\ell + 1/2)^6} \right) \right\}. \end{aligned} \quad (39b)$$

For $\mu = 0$, formula (39) is in agreement with Eq. (7) and Eqs. (17)-(22) of Ref. [47].

III. CAM DESCRIPTION OF THE HIGH-ENERGY ABSORPTION CROSS SECTION AND ROLE OF THE MASS

A. Generalities

In this section, we shall focus our attention on the absorption cross section defined by (14) (see also Refs. [32, 43] for previous numerical investigations). We shall more particularly provide a simple and very accurate approximation of this series emphasizing the role of the mass parameter μ and permitting us to describe qualitatively and quantitatively its behavior for high frequencies/energies.

With this aim in mind, it is necessary to replace the sum over the partial waves (14) by the series over Regge poles

$$\begin{aligned} \sigma_{\text{abs}}(\omega) &= \sigma_{\text{geo}}(\omega) \\ &- \frac{4\pi^2}{[p(\omega)]^2} \text{Re} \left(\sum_{n=1}^{+\infty} \frac{e^{i\pi[\lambda_n(\omega)-1/2]} \lambda_n(\omega) \gamma_n(\omega)}{\sin[\pi(\lambda_n(\omega) - 1/2)]} \right) \\ &+ \dots \end{aligned} \quad (40)$$

In Eq. (40), $\sigma_{\text{geo}}(\omega)$ is the geometrical cross section of the black hole given by (5) and the $\lambda_n(\omega)$ with $n \in \mathbb{N} \setminus \{0\}$ are those of the (Regge) poles of the analytic extension $\Gamma_{\lambda-1/2}(\omega)$ of the greybody factor $\Gamma_\ell(\omega)$ lying in the first quadrant of the complex λ plane while the $\gamma_n(\omega)$ are the associated residues. We can obtain (40) from (14) by using the CAM machinery and by repeating for $\omega > \mu$, *mutatis mutandis*, the main steps of Sec. II of Ref. [14] where we considered the absorption cross section for a

massless scalar field. This is possible due to the properties of the Regge poles and of the analytic extension of the T -matrix mentioned in Sec. II.A. In Eq. (40), the dots are associated with a background integral along the imaginary λ axis. We shall assume that it can be neglected numerically and physically at high energies.

It is now possible to consider the high-energy behavior of the absorption cross section (14) by replacing into (40) the functions $\lambda_n(\omega)$ and $\gamma_n(\omega)$ by their high-frequency asymptotic expansions. We have already at our disposal the expansion (26) for the Regge poles $\lambda_n(\omega)$. It remains to us to construct the analogous expansions for the residues $\gamma_n(\omega)$.

B. Regge-pole residues of the greybody factors

It should be first noted that the Dolan-Ottewill method we have found very efficient for the construction of the high-frequency asymptotic expansion of the Regge poles cannot be naturally adapted to the determination of the residue asymptotic expansions (see also a remark below). However, it is possible to achieve such a job very efficiently from the WKB approach of Sec. II.C.

The Regge poles are the poles of the analytic extension $\Gamma_{\lambda-1/2}(\omega)$ of the greybody factors given by (34) and the solutions of Eq. (35). As a consequence, it is easy to prove that the corresponding residues are given by

$$\gamma_n(\omega) = \frac{-1/2}{[d\mathcal{S}_{\lambda-1/2}(\omega)/d\lambda]_{\lambda=\lambda_n(\omega)}}. \quad (41)$$

Then, from (41), (28), (17b) and (26), we obtain the asymptotic expansion (a fifth-order WKB approximation)

$$\begin{aligned} \gamma_n(\omega) &= -\frac{1}{2\pi} + i\alpha(n) \left[\frac{5}{36\pi} \right] \left(\frac{1}{3\sqrt{3}M\omega} \right) + \left[\frac{305}{2592\pi} \alpha^2(n) - \frac{1357 - 46656M^2\mu^2}{31104\pi} \right] \left(\frac{1}{(3\sqrt{3}M\omega)^2} \right) \\ &+ i\alpha(n) \left[\frac{49115}{419904\pi} \alpha^2(n) - \frac{192917 - 1189728M^2\mu^2}{1679616\pi} \right] \left(\frac{1}{(3\sqrt{3}M\omega)^3} \right) \\ &+ \left[-\frac{15095915}{120932352\pi} \alpha^4(n) + \frac{18327325 - 54867456M^2\mu^2}{80621568\pi} \alpha^2(n) \right. \\ &\quad \left. - \frac{28395953 + 611380224M^2\mu^2 - 117546246144M^4\mu^4}{5804752896\pi} \right] \left(\frac{1}{(3\sqrt{3}M\omega)^4} \right) + \mathcal{O}_{M\omega \rightarrow +\infty} \left(\frac{1}{(3\sqrt{3}M\omega)^5} \right). \end{aligned} \quad (42)$$

It is interesting to note that, in a very recent article [63], Dolan and Ottewill have developed new techniques based on their ansatz in order to construct analytically the black hole excitation factors associated with the complex quasinormal frequencies. Their techniques could be adapted to obtain the two first terms of (42) but, unfor-

tunately, this requires lot of work.

C. CAM approximation for the absorption cross section

Let us now insert (26) and (42) into (40) and take into account Eq. (6c). By noting that the contribution of the

Regge poles with $n > 1$ is practically negligible and that, for mathematical coherence, we only need the first three terms of (26) and the first two terms of (42), we obtain

$$\sigma_{\text{abs}}(\omega) \approx 27\pi M^2 \left(1 + \frac{2\mu^2}{3\omega^2} - 8\pi e^{-\pi} \frac{\sin[2\pi(3\sqrt{3}M)\omega]}{2\pi(3\sqrt{3}M)\omega} + 16\pi e^{-2\pi} \frac{\sin[4\pi(3\sqrt{3}M)\omega]}{4\pi(3\sqrt{3}M)\omega} + \frac{4\pi^2 e^{-\pi} [-39 + 7\pi + 972\pi M^2 \mu^2] \cos[2\pi(3\sqrt{3}M)\omega]}{27 [2\pi(3\sqrt{3}M)\omega]^2} \right). \quad (43)$$

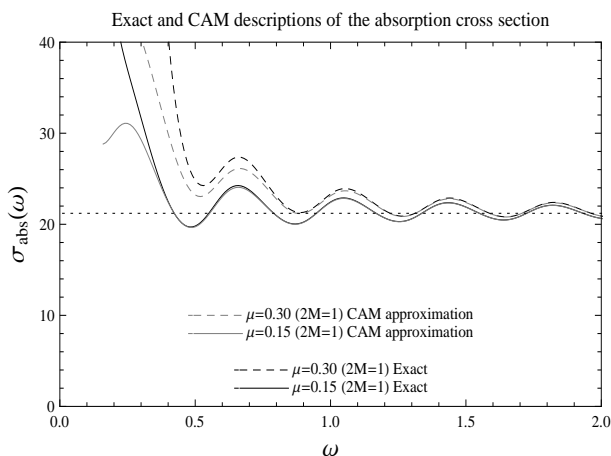


FIG. 2: The exact absorption cross section (14) and its CAM approximation (45) are compared for $\mu = 0.15$ and $\mu = 0.30$ ($2M = 1$). The limiting constant value $27\pi M^2$ corresponding to the geometrical cross section of the photon sphere is also indicated.

For $\mu = 0$, formula (43) reduces to Eq. (2.12) of Ref. [64] and is the superposition of an eikonal contribution (see also Ref. [14]) and a fine structure. It is interesting to recall that the eikonal contribution is the sum of the geometrical cross section of the black hole photon sphere and a sinc function involving the geometrical characteristics (orbital period and Lyapunov exponent) of the null unstable geodesics lying on this photon sphere. It describes accurately the high-energy behavior of the absorption cross section and, in particular, of its regular and attenuated oscillations around a limiting value (see, e.g., Ref. [65] for a numerical analysis of this behavior obtained a long time ago). The fine structure is a slightly more complicated function which also involves the geometrical characteristics of the null unstable geodesics lying on the photon sphere and which, above all, permits us to capture small fluctuations lying beyond the eikonal contribution. For $\mu \neq 0$, even if it is

not so natural, an analogous description can be provided: we can associated the first three terms of (43), i.e.,

$$\sigma_{\text{abs}}^{\text{Eik}}(\omega) \equiv 27\pi M^2 \left(1 + \frac{2\mu^2}{3\omega^2} - 8\pi e^{-\pi} \frac{\sin[2\pi(3\sqrt{3}M)\omega]}{2\pi(3\sqrt{3}M)\omega} \right) \quad (44)$$

with the eikonal description and the two last ones, i.e.,

$$27\pi M^2 \left[16\pi e^{-2\pi} \frac{\sin[4\pi(3\sqrt{3}M)\omega]}{4\pi(3\sqrt{3}M)\omega} + \frac{4\pi^2 e^{-\pi} [-39 + 7\pi + 972\pi M^2 \mu^2] \cos[2\pi(3\sqrt{3}M)\omega]}{27 [2\pi(3\sqrt{3}M)\omega]^2} \right] \quad (45)$$

with the fine structure. We can observe that the mass parameter μ appears in both contributions, greatly modifies the eikonal part and slightly corrects the amplitude of one of the terms (the smallest one for very high frequencies) of the fine structure.

We have tested numerically formula (43). It describes very accurately the absorption cross section (14) as well as its oscillations around the geometrical cross section and, in particular, it takes into account very correctly the contributions of the mass parameter μ . In Fig. 2, for two values of the mass parameter μ , we have displayed the exact absorption cross section numerically obtained from (14) by solving the problem defined by (7), (8) and (9) and we have compared it with the result provided by (43). The agreement is remarkable even for rather low energies. We can however observe that, for low energies, the accuracy of the CAM description decreases when the mass parameter μ increases. Moreover, it should be noted that our numerical absorption cross sections seem to be in agreement with those of Ref. [43] but totally disagree with those displayed in Ref. [32].

In Fig. 3, for the same values of the mass parameter μ , we have also tested the accuracy of the CAM description

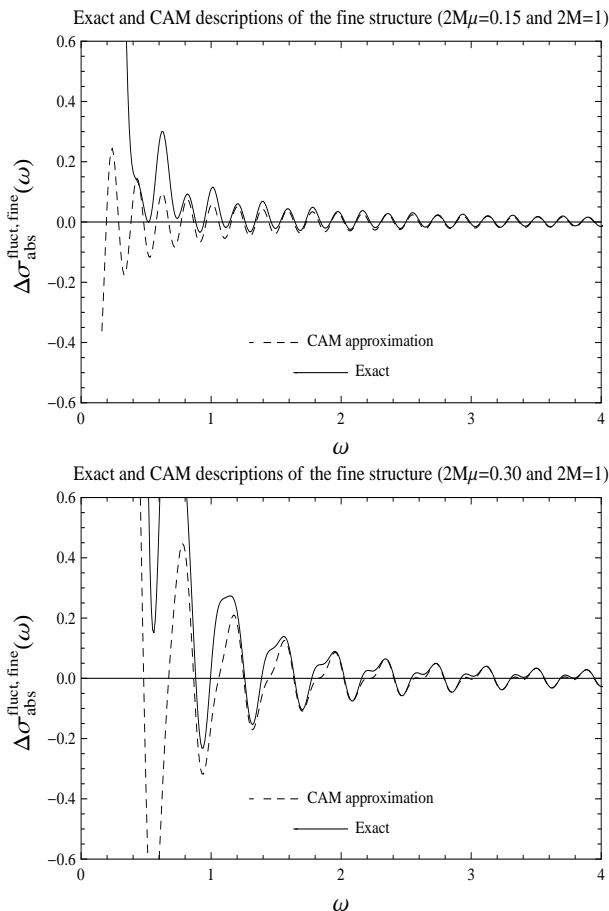


FIG. 3: Fine structure for $\mu = 0.15$ and $\mu = 0.30$ ($2M = 1$). We compare the exact fine structure (46) with its CAM approximation (45).

(45) of the exact fine structure defined by

$$\Delta\sigma_{\text{abs}}^{\text{fluct, fine}}(\omega) \equiv \sigma_{\text{abs}}(\omega) - \left[27\pi M^2 \left(1 + \frac{2\mu^2}{3\omega^2} - 8\pi e^{-\pi} \frac{\sin[2\pi(3\sqrt{3}M)\omega]}{2\pi(3\sqrt{3}M)\omega} \right) \right] \quad (46)$$

and numerically calculated. The agreement is remarkable for high frequencies and remains robust even for rather

low ones. It should be noted that the behavior of the fine structure is very simple for $2M\mu = 0.15$ because, in this case, the coefficient of the second term in Eq. (45) can be neglected. In fact, it vanishes for $2M\mu \approx 0.149265\dots$

IV. CONCLUSION AND PERSPECTIVES

In the present paper, by working in the CAM plane, we have emphasized explicitly the role of the mass parameter in the resonance and absorption spectra of the Schwarzschild black hole for massive scalar perturbations and simplified considerably their description. Our work could be extended to the case of the massive scalar field propagating on the Reissner-Nordström, Kerr and Kerr-Newmann black holes as well as to the more interesting case, from a physical point of view, of massive fermions [19]. This last problem could even have nice applications in the context of multimessenger high-energy astrophysics. With this aim in view, the recent articles by Dolan, Doran, Lasenby and coworkers [12, 37, 38] would constitute a natural and solid starting point.

It is finally important to point out that, in this paper, the Regge pole machinery has not permitted us to understand the existence of the bound state spectrum [16, 20, 23, 25, 26, 36, 43] associated with the massive scalar field theory defined on the Schwarzschild black hole. This is really a pity and we consider that it is one of the crucial problems to be tackled in the framework of CAM techniques. Indeed, if we could solve such a problem, we could maybe provide a dual simple explanation of the realization by massive fields of the so-called “black hole bomb” scenario [66] or, in other words, of the instabilities induced by the bound state spectrum in the presence of rotation and due to the superradiance phenomenon (see, e.g., Refs. [17, 18, 21, 22, 34, 35, 39, 42]).

Acknowledgments

We are grateful to Alexei Starobinsky for information concerning the Russian literature and for having pointed to our attention Refs. [20] and [23]. We also thank Sam Dolan for providing us with recent references on black hole instabilities.

-
- [1] R. A. Matzner, *J. Math. Phys.* **9**, 163 (1968).
 - [2] W. W. Hildreth, *Ph. D. Thesis* (Princeton University, Unpublished, 1964).
 - [3] R. G. Newton, *Scattering Theory of Waves and Particles* (Springer-Verlag, New York, 1982), 2nd ed.
 - [4] J. A. H. Futterman, F. A. Handler, and R. A. Matzner, *Scattering from black holes* (Cambridge University Press, Cambridge, 1988).
 - [5] P. Anninos, C. DeWitt-Morette, R. A. Matzner,

- P. Yioutas, and T. R. Zhang, *Phys. Rev. D* **46**, 4477 (1992).
- [6] N. Andersson and K.-E. Thylwe, *Class. Quantum Grav.* **11**, 2991 (1994).
- [7] N. Andersson, *Class. Quantum Grav.* **11**, 3003 (1994).
- [8] S. R. Das, G. W. Gibbons, and S. D. Mathur, *Phys. Rev. Lett.* **78**, 417 (1997).
- [9] J. Maldacena and A. Strominger, *Phys. Rev. D* **56**, 4975 (1997).

- [10] K. Glampedakis and N. Andersson, *Class. Quantum Grav.* **18**, 1939 (2001).
- [11] V. Cardoso, O. J. C. Dias, J. P. S. Lemos, and S. Yoshida, *Phys. Rev. D* **70**, 044039 (2004).
- [12] S. Dolan, C. Doran, and A. Lasenby, *Phys. Rev. D* **74**, 064005 (2006).
- [13] L. C. B. Crispino, S. Dolan, and E. S. Oliveira, *Phys. Rev. Lett.* **102**, 231103 (2009).
- [14] Y. Décanini, G. Esposito-Farèse, and A. Folacci, *Phys. Rev. D* **83**, 044032 (2011).
- [15] P. A. Collins, R. Delbourgo, and R. M. Williams, *J. Phys. A: Math. Nucl. Gen.* **6**, 161 (1973).
- [16] N. Deruelle and R. Ruffini, *Phys. Lett. B* **52**, 437 (1974).
- [17] N. Deruelle and R. Ruffini, *Phys. Lett. B* **57**, 248 (1975).
- [18] T. Damour, N. Deruelle, and R. Ruffini, *Lett. Nuovo Cimento* **15**, 257 (1976).
- [19] W. G. Unruh, *Phys. Rev. D* **14**, 3251 (1976).
- [20] I. M. Ternov, V. P. Halilov, G. A. Chizhov, and A. B. Gaina, *Izv. Vuz. USSR Fiz.* **21**, 109 (1978).
- [21] T. M. Zouros and D. M. Eardley, *Ann. Phys.* **118**, 139 (1979).
- [22] S. Detweiler, *Phys. Rev. D* **22**, 2323 (1980).
- [23] L. A. Kofman, *Phys. Lett. A* **87**, 281 (1982).
- [24] A. B. Gaina, *Sov. Phys. JETP* **69**, 13 (1989).
- [25] O. B. Zaslavskii, *Class. Quantum Grav.* **7**, 589 (1990).
- [26] L. E. Simone and C. M. Will, *Class. Quantum Grav.* **9**, 963 (1992).
- [27] H. Koyama and A. Tomimatsu, *Phys. Rev. D* **63**, 064032 (2001).
- [28] H. Koyama and A. Tomimatsu, *Phys. Rev. D* **64**, 044014 (2001).
- [29] R. A. Konoplya, *Phys. Lett. B* **550**, 117 (2002).
- [30] L. Xue, B. Wang, and R.-K. Su, *Phys. Rev. D* **66**, 024032 (2002).
- [31] L. M. Burko and G. Khanna, *Phys. Rev. D* **70**, 044018 (2004).
- [32] E. Jung and D. K. Park, *Class. Quantum Grav.* **21**, 3717 (2004).
- [33] A. Ohashi and M. Sakagami, *Class. Quantum Grav.* **21**, 3973 (2004).
- [34] H. Furuhashi and Y. Nambu, *Prog. Theor. Phys.* **112**, 983 (2004).
- [35] M. J. Strafuss and G. Khanna, *Phys. Rev. D* **71**, 024034 (2005).
- [36] R. A. Konoplya and A. V. Zhidenko, *Phys. Lett. B* **609**, 377 (2005).
- [37] C. Doran, A. Lasenby, S. Dolan, and I. Hinder, *Phys. Rev. D* **71**, 124020 (2005).
- [38] A. Lasenby, C. Doran, J. Pritchard, A. Caceres, and S. Dolan, *Phys. Rev. D* **72**, 105014 (2005).
- [39] V. Cardoso and S. Yoshida, *J. High Energy Phys.* **07**, 009 (2005).
- [40] R. A. Konoplya, *Phys. Rev. D* **73**, 024009 (2006).
- [41] R. A. Konoplya, A. V. Zhidenko, and C. Molina, *Phys. Rev. D* **75**, 084004 (2007).
- [42] S. Dolan, *Phys. Rev. D* **76**, 084001 (2007).
- [43] J. Grain and A. Barrau, *Eur. Phys. J. C* **53**, 641 (2008).
- [44] S. Hod, *Phys. Rev. D* **84**, 044046 (2011).
- [45] Y. Décanini, A. Folacci, and B. P. Jensen, *Phys. Rev. D* **67**, 124017 (2003).
- [46] Y. Décanini and A. Folacci, *Phys. Rev. D* **79**, 044021 (2009).
- [47] S. Dolan and A. C. Ottewill, *Class. Quantum Grav.* **26**, 225003 (2009).
- [48] Y. Décanini and A. Folacci, *Phys. Rev. D* **81**, 024031 (2010).
- [49] Y. Décanini, A. Folacci, and B. Raffaelli, *Phys. Rev. D* **81**, 104039 (2010).
- [50] S. Dolan, L. A. Oliveira, and L. C. B. Crispino (2011), arXiv:1105.1795 [gr-qc].
- [51] B. F. Schutz and C. M. Will, *Astrophys. J.* **291**, L33 (1985).
- [52] S. Iyer and C. M. Will, *Phys. Rev. D* **35**, 3621 (1987).
- [53] S. Iyer, *Phys. Rev. D* **35**, 3632 (1987).
- [54] C. M. Will and J. W. Guinn, *Phys. Rev. A* **37**, 3674 (1988).
- [55] R. A. Konoplya, *Phys. Rev. D* **68**, 024018 (2003).
- [56] C. W. Misner, K. S. Thorne, and J. A. Wheeler, *Gravitation* (W. H. Freeman and Company, San Francisco, 1973).
- [57] S. Chandrasekhar, *The Mathematical Theory of Black Holes* (Oxford University Press, Oxford, 1983).
- [58] D. G. Boulware, *Phys. Rev. D* **11**, 1404 (1975).
- [59] B. S. DeWitt, *The Global Approach to Quantum Field Theory* (Oxford University Press, Oxford, 2003).
- [60] V. P. Frolov and I. D. Novikov, *Black Hole Physics* (Kluwer Academic Publishers, Dordrecht, 1998).
- [61] E. W. Leaver, *Proc. R. Soc. London A* **402**, 285 (1985).
- [62] B. Majumdar and N. Panchapakesan, *Phys. Rev. D* **40**, 2568 (1989).
- [63] S. Dolan and A. C. Ottewill (2011), arXiv:1106.4318 [gr-qc].
- [64] Y. Décanini, A. Folacci, and B. Raffaelli, *Class. Quantum Grav.* **28**, 175021 (2011).
- [65] N. Sánchez, *Phys. Rev. D* **18**, 1030 (1978).
- [66] W. H. Press and S. A. Teukolsky, *Nature* **238**, 211 (1972).